The effect of cyclodextrins on the aqueous solubility of a new MMP inhibitor: phase solubility, ^{1}H-NMR spectroscopy and molecular modeling studies, preparation and stability study of nebulizable solutions.

Bertholet Pascal[1*], Gueders Maud[2*], Dive Georges[3], Albert Adelin[4], Barillaro Valery[1], Perly Bruno[5], Cataldo Didier[2], Piel Géraldine[1], Delattre Luc[1], Evrard Brigitte[1]

[1]Laboratory of Pharmaceutical Technology, Department of Pharmacy, University of Liège, Belgium
[2]Laboratory of Tumors and Development Biology, University of Liège, Belgium
[3]Center for Protein Engineering, Chemical Department, University of Liège, Belgium
[4]Biostatistics Department, University of Liège, Belgium
[5]Laboratory of Molecular Chemistry, Gif-Sur-Yvette Cedex, France
[*]Equal contributors to this study.

Received 14 January 2005, Revised 22 February 2005, Accepted 28 February 2005, Published 14 July 2005

Abstract PURPOSE Ro 28-2653 (RO) is a synthetic inhibitor of matrix metalloproteinases (MMPs), which is potentially effective against bronchial remodeling. Given that this molecule has very poor aqueous solubility, different cyclodextrins (CDs) have been tested to increase its solubility. The aim of this study was to prepare and to characterize inclusion complexes between RO and CDs, in order to develop nebulizable solutions. **METHODS** The complex formation was investigated by phase solubility studies. ^{1}H-NMR spectroscopy and molecular modeling studies were carried out to elucidate the structure of the inclusion complex between RO and dimethyl-β-CD (DIMEB). Nebulizable solutions of RO were developed with CDs and a stability study was performed over 9 months. **RESULTS** The phase solubility studies showed that β-CD and its derivatives form a 1:2 complex with RO, whereas γ-CD includes RO with a 1:1 stoichiometry and a weak stability constant. T-ROESY spectra showed that DIMEB is able to complex two RO substituents (nitrophenyl and biphenyl groups) with preferential orientations, while molecular modeling demonstrated that the configurations observed with ^{1}H-NMR are energetically favorable, especially owing to H-bond formation between RO and DIMEB. Two CDs were selected to develop nebulizable solutions of RO and the stability study demonstrated that RO degradation in solution is strongly dependent on the concentration of the 1:2 inclusion complex.

CONCLUSIONS CDs are able to include RO and to improve its aqueous solubility. The β-CD derivatives can be used to formulate nebulizable solutions of RO, the stability of which depends on the concentration of the 1:2 complex.

Corresponding Author: Bertholet Pascal, Laboratory of Pharmaceutical Technology, Department of Pharmacy, University of Liège, Belgium. p.bertholet@ulg.ac.be

INTRODUCTION

Matrix metalloproteinases (MMPs) are zinc-dependent proteolytic enzymes able to break down basement membranes and most extracellular matrix components (1). The expression and activation of MMPs are carefully regulated in physiological conditions in order to prevent uncontrolled destruction of body tissues, but this regulation may be modified or disrupted in many pathological processes (2-6). Asthma is a chronic inflammatory disease characterized by bronchial hyperresponsiveness and profound extracellular matrix changes that are collectively referred to as bronchial remodeling (7, 8). It has been demonstrated that overexpression of some MMPs into asthmatic airways (especially MMP-2 and MMP-9) is involved in bronchial remodeling (9-11). For these conditions, a specific inhibition of both MMPs could lead to a new therapeutic approach for asthma (12, 13).

Ro 28-2653 (RO), a barbituric derivative (Figure 1), is a synthetic inhibitor of MMPs with a high selectivity for MMP-2, MMP-9 and MMP-14 (14). As its effectiveness has already been demonstrated in disease models with MMP-9 expression disorders (15, 16), RO should be effective against bronchial remodeling.

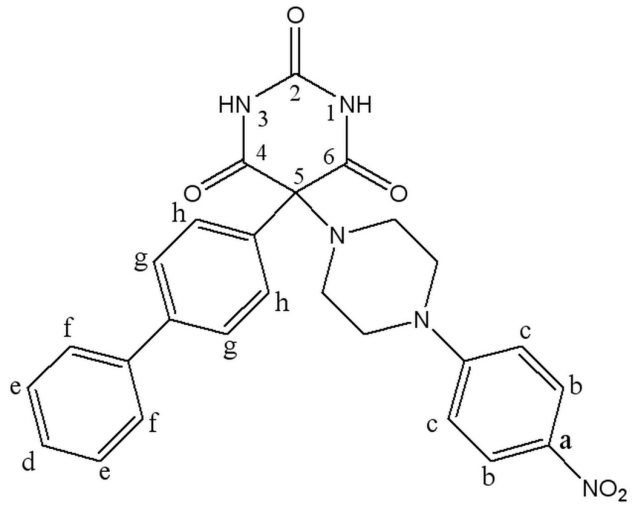

Figure 1: Chemical structure of Ro 28-2653.

The inhalation route is widely studied for many drug applications focusing on local distribution. The poor solubility of active substances poses problems, for example, the aqueous solubility of RO (< 1µg/ml) does not allow the exploration of large concentration ranges and corresponding pharmacological responses. Rather than using co-solvents, which can be irritant or toxic after inhalation (17, 18), cyclodextrins (CDs) have been tested to increase RO aqueous solubility and to develop nebulizable solutions. CDs are cyclic oligosaccharides consisting of α 1-4 linked glucopyranose units with a hydrophilic outer surface and a lipophilic cavity, which is able to include some organic molecules by non-covalent interaction forces. In the pharmaceutical field, CDs are used to enhance solubility, dissolution rate and bioavailability of insoluble drugs (19, 20).

The feasibility of using different CDs to elaborate pharmaceutical formulations for the inhalation route has previously been demonstrated and short-term toxicity of these solutions on C57BL/6 has been tested (21).

The effect of different CDs on the aqueous solubility and on the chemical stability of RO was investigated by phase solubility studies and by ^{1}H-NMR spectroscopy and molecular modeling studies, with the aim of preparing stable and effective nebulizable solutions.

MATERIALS AND METHODS

Materials

RO was synthetized by Syntheval (Caen, France) according to patent WO9858925. Hydroxypropyl-β-CD (HP-β-CD, Kleptose HPB^R) (Eur. Ph. 4th Edition, 3.22% H_2O, D.S. 0.62) and β-CD (Kleptose^R) (Eur. Ph. 4th Edition, 7.58% of H_2O) were provided by Roquette (Lestrem, France). Randomly methylated-β-CD (RAMEB) (2.7% H_2O, D.S. 1.7) and γ-CD (7.7% H_2O) were generously given by Wacker Chemie GmbH (Munich, Germany). 2, 6-dimethyl-β-CD (DIMEB) was synthesized by CEA (Saclay, France) and was highly purified by extensive preparative chromatography. Apyrogenic phosphate buffered saline (PBS) and water for injection were purchased from Bio-Wittaker (Verviers, Belgium). Cyclodextrins and RO were tested following the Bacterial Endotoxin Test described in USP XXVI using Limulus Amebocyte Lysate (LAL). All the other reagents were of analytical grade.

Assay of RO

The RO concentration was assayed by an HPLC method. The HPLC system consisted of an L-7100 Merck-Hitachi pressure pump, an L-7200 Merck-Hitachi autosampler, an L-7350 Merck-Hitachi column oven, an L-7455 Merck-Hitachi diode array detector and a D-7000 interface. The system was controlled by a computer running the "HPLC System Manager v 4.0" acquisition software developed by Merck-Hitachi. Twenty-µl samples were injected on a Lichrocart column (125 x 4 mm i.d.) prepared with a Lichrospher 60 RP-Select B 5 µm phase (Merck) and the temperature was maintained at 30°C. The mobile phase consisted of a 70:30 (v/v) mixture of methanol (HPLC grade) and a 0.05 M potassium dihydrogenphosphate buffer (pH3). The flow rate was adjusted to 1.0 mL/min. All samples were analyzed in duplicate at 265 nm. This method was successfully validated and showed good linearity, reproducibility and accuracy between 4 and 20 µg/ml. The limits of detection (LOD) and of quantification (LOQ) were both determined and found to be equal to 0.083 µg/mL and to 0.28 µg/mL respectively.

Phase solubility studies

Solubility studies were performed as described by Higuchi and Connors (22). Excess amounts of RO were added to aqueous CD solutions of increasing con-

centration. The tested CDs were β-CD (0, 2, 4, 8, 10, 12, 16 mM), γ-CD (0, 10, 25, 50, 75, 100, 150 mM), RAMEB and HP-β-CD (0, 10, 25, 50, 75, 100, 150, 200 mM). After shaking at 37°C for 7 days, the undissolved RO was removed by filtration through a 0.45 μm filter (Millex-HV, Millipore) and the solutions were assayed for RO content by HPLC.

^{1}*H-NMR spectroscopy studies*

The ^{1}H-NMR spectrum of RO in D_2O could not be performed due to its very low aqueous solubility, therefore ^{1}H-NMR signal assignments for RO were performed in DMSO. Solutions containing RO and DIMEB were prepared as follows: an excess amount of RO was added to a 10 mM Dimeb D_2O solution. After shaking for 7 days at 37°C, the suspension was filtered (Millex-HV, Millipore). All ^{1}H-NMR experiments were performed on a Bruker DRX500 spectrometer operating at 500 MHz for protons. The temperature was set at 25°C. Calibration was achieved using the residual resonance of the solvent as secondary reference (4.80 ppm for HDO) corresponding to external TMS at 0 ppm. For T-ROESY experiments, a 300-msec mixing time was used. All processings were carried out on a Silicon Graphics INDY data station using the WINNMR program from Bruker.

Molecular modeling

Calculations were performed at the approximate quantum chemistry AM1 level using the Gaussian 98 suite of programs (23). The thermochemical results at 298.15°K and 1 atm were computed from the numerically derived frequencies using statistical mechanics formulas (24). The same procedure had been used in previous studies on miconazole and cyproterone acetate inclusion complexes (25, 26). Starting from the optimized geometry local minimum of each complex, RO and CDs were re-optimized separately. This procedure allows the determination of consistent energetic data, as each relative energy is calculated by reference to the geometry of the complex. Interatomic distances were measured by Mercury 1.2.1 Software (Cambridge, U.K.).

Formulation of RO nebulizable solution

Nebulizable solutions were formulated with RO in water for injection; at a concentration of 30 and 300 μg/ml. Suitable amounts of RO were added. In order to decrease the required time for inclusion, freshly prepared suspensions were heated in an autoclave at 120°C for 30 minutes. After this treatment, an HPLC analysis was performed in order to check possible RO degradation. Osmolality of the solutions was measured by a Knauer Automatic semi-micro Osmometer (Chromspec, Canada) and adjusted to the value of 286 mOsm/kg by addition of a sufficient amount of NaCl. Terminal sterilization of the solutions was performed by a steam sterilization process.

The distribution of aerosol sprayed droplets emitted from RO solutions was determined with a laser size analyzer Mastersizer (Malvern, Orsay, France). Ten milliliters of each solution were directly nebulized in the laser beam. The mouthpiece was held at 1 cm from the center of the laser beam. The resulting aerosol was aspirated on the opposite side of the beam. Environmental temperature and relative humidity were maintained constant, which is to say at 20°C and 40-45% RH. Each experiment was carried out in triplicate. The results are expressed as the median diameter of droplets and the percentage of droplets in the range of 0.5 – 5.8 μm. The concentration of droplets in the air evaluated by the obscuration percentage of the laser beam was in the same range for each experiment (15-25%). The RO solution aerosol was produced by using an ultrasonic nebulizer SYSTAM (Système Assistance Medical, Le Ledat, France), the vibration frequency of which is 2.4 MHz, with variable vibration intensity and ventilation levels. Vibration intensity was fixed in position 6 and the ventilation level was 25 L/min.

RO chemical stability in nebulizable solutions was investigated according to the European Guidelines (27). For each formulation, three independent batches were prepared. One mL aliquot samples were stored at two temperatures (4 and 25°C). RO content was determined by the previously described HPLC method after 7 days, 1, 3, 6 and 9 months. The effect of time, temperature, type and concentration of CD, as well as their interaction with the RO concentration, was tested by means of the general linear mixed model. This accounts for repeated observations on the sample units. All results were considered to be significant at the 5% critical level ($p < 0.05$). Statistical analyses were carried out using SAS (version 8.2 for Windows). The solutions were also checked visually for the absence of precipitation.

Table 1: Stoichiometry and stability constant of RO-CD complexes in water.

CD	Type of diagram	Stoichiometry	$K_{1:1}$ (M^{-1})	$K_{1:2}$ (M^{-1})
β-CD	B_S	1:1, 1:2	2092	-
γ-CD	A_L	1:1	346	-
HP-β-CD	A_P	1:1, 1:2	12575	14.4
RAMEB	A_P	1:1, 1:2	27595	22.9

RESULTS AND DISCUSSION

Phase solubility studies

Figure 2 shows diagrams obtained with the different CDs. β-CD and γ-CD show a very slight increase of RO aqueous solubility, whereas solubility increases much more using β-CD derivatives HP-β-CD and RAMEB). The most significant increase was observed with RAMEB.

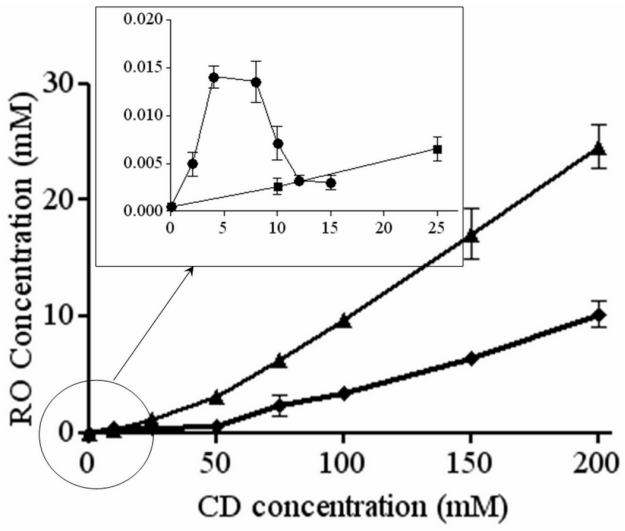

Figure 2: Phase solubility diagrams of RO with β-CD (•), γ-CD (■), RAMEB (▲) and HP-β-CD (↵). In the frame, an enlargement of the RO solubility profile obtained with β-CD.

According to Higuchi and Connors (22), β-CD shows a B_S diagram. From 0 to 4 mM β-CD concentration, the apparent solubility of RO is increased due to the formation of a soluble complex. As the ascending portion of this diagram may be considered as an A_L type diagram, it is possible to determine the complex stoichiometry.

As the slope value is less than 1 ($2.4\ 10^{-3}$), it could be considered as a 1:1 complex. At the β-CD concentration value of 4 mM, the solubility limit of this complex is reached (6.8 μg/mL). Further β-CD addition results in the precipitation of the complex. From 8 mM β-CD concentration, RO solubility decreases to reach a plateau. Because of RO excess, this decrease cannot be explained by its depletion in solution. These observations suggest that β-CD adding above 8 mM forms another complex with a different stoichiometry (probably 1:2) and a lowest solubility (1.5 μg/mL).

The stability constant of the 1:1 complex may be calculated by the ascending part of the diagram by equation 1 and this is given in Table 1.

$$K_{1:1} = \frac{Slope}{S_0.(1-Slope)} \quad M^{-1} \qquad \text{Eq.1}$$

where S_o corresponds to aqueous solubility of RO (0.56 μg/ml) without CD.

The γ-CD shows an A_L diagram ($r^2=0.99$), and because the slope is lower than 1 (4.10^{-4}), the complex stoichiometry is most probably 1:1. The stability constant is determined by equation 1. The low stability constant value means that interactions between RO and γ-CD are weak, probably because the CD cavity is too large to include RO tightly. HP-β-CD and RAMEB diagrams are classified as A_P diagrams. In order to determine the stoichiometry of the complexes with HP-β-CD and RAMEB,

St-So/[CD]t-(St-So)

was plotted as a function of ($[CD]_t$-(S_t-S_0)) (Figure 3).

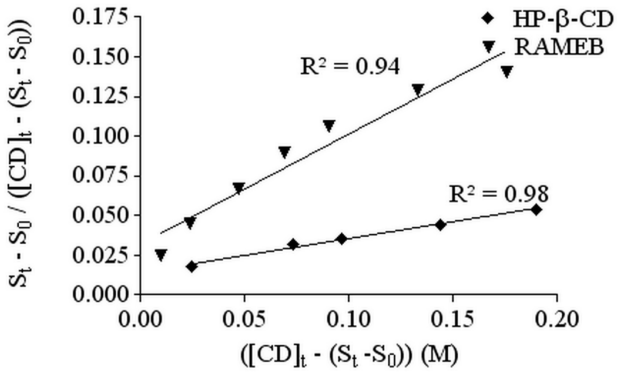

Figure 3: Representation of ($[CD]_t$-(S_t-S_0)) in function of St-So/[CD]t-(St-So) to determine the stoichiometry and the stability constant of the Ro 28-2653 complex with RAMEB (▲) and HP-β-CD (◆).

Both cyclodextrins show a straight line, which means that these CDs form complexes with RO of 1:1 and 1:2 stoichiometries. Stability constants ($K_{1:1}$, $K_{1:2}$) were calculated by solving equation 2 and are reported in Table 1.

$$\frac{S_t - S_0}{[CD]_t - (S_t - S_0)} = K_{1:1}.S_0 + K_{1:1}.K_{1:2}.S_0.([CD]_t - (S_t - S_0)) \qquad \text{Eq.2}$$

where S_t and $[CD]_t$ correspond to total RO and CD concentration respectively.

According to the important aqueous solubility increase, both complexes display a very high $K_{1:1}$ value (more than 10,000 M^{-1}). The apparent low value of $K_{1:2}$ does not have to be interpreted as an unfavorable 1:2 complex formation. Indeed, the 1:1 and 1:2 complex ratios depend on CD concentration and may be calculated by solving the equation system 3:

$$K_{1:1} = \frac{[CD.RO]}{[RO].[CD]} \quad M^{-1} \qquad \text{Eq.3}$$

$$K_{1:2} = \frac{[CD_2.RO]}{[CD.RO].[CD]} \quad M^{-1}$$

Where:
[RO] = uncomplexed RO concentration
[CD] = uncomplexed CD concentration
[CD.RO] = 1:1 complex concentration

For example, if the RAMEB concentration is equal to 200 mM, the 1:1 and 1:2 complexes concentration will correspond to 5.04 mM and 18.28 mM respectively.

^{1}*H-NMR spectroscopy studies*

As methylated β-CD seems to give the highest increase in solubility, further investigations of the chemical structure of the complex were undertaken with DIMEB, a pure methylated-β-CD derivative which allows to obtain a high resolution spectrum from which all protons can be assigned contrary to RAMEB. The spectrum of pure DIMEB was compared with the spectrum of DIMEB in the presence of RO (Figure 4).

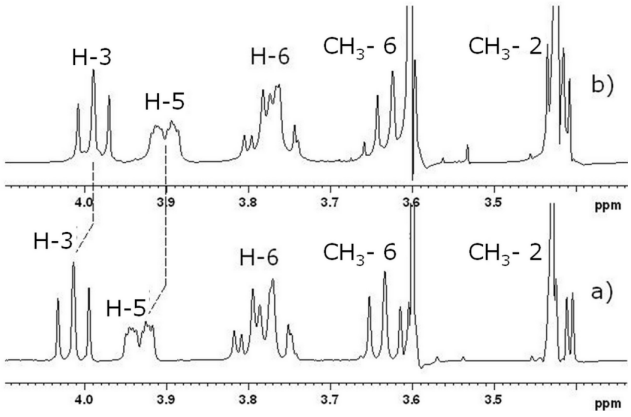

Figure 4: Partial ^{1}H-NMR spectra of 10 mM solutions (a) DIMEB in presence of RO and (b) DIMEB in D_2O with assignment of the signals of the CD.

The signals corresponding to H-3 and H-5 protons were shifted upfield. Because these protons are inside the cyclodextrin cavity, their shift suggests that RO or part of RO is included inside the DIMEB (23). T-ROESY spectra were performed to provide more information on the structure of the complex (Figure 5).

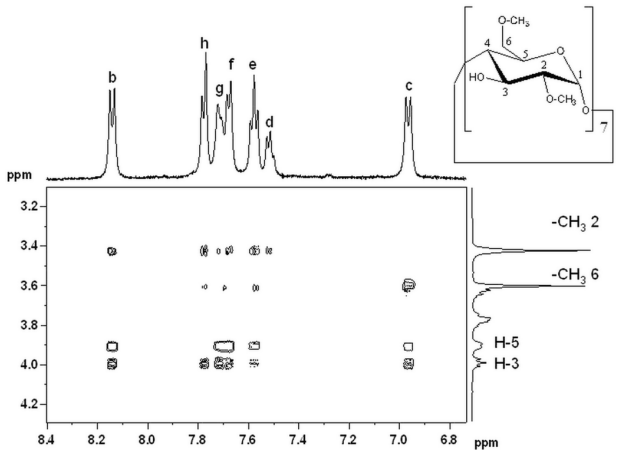

Figure 5: Contour plot of T-ROESY spectrum of RO dissolved in a 10 mM DIMEB solution in D_2O.

Correlation spots indicated interactions between b, c, e, f, g and h RO protons and H-3 and H-5. Other interactions between RO protons and DIMEB $-CH_3$ 6* and 2* (corresponding to primary and secondary hydroxyl faces respectively) were observed. On the one hand, H-b only interfered with $-CH_3$2*, whereas H-c only showed correlation spots with $-CH_3$6*. On the other hand, all biphenyl protons interfered with $-CH_3$2* and 6*. All these observations suggest that both barbituric substituents of RO are complexed by DIMEB.

The nitrophenyl group is included by DIMEB with primary hydroxyls oriented towards the piperazin cycle, whereas the biphenyl group is included by a second DIMEB molecule, but with two possible inclusion directions, primary or secondary hydroxyls oriented towards the barbituric ring (Figure 6).

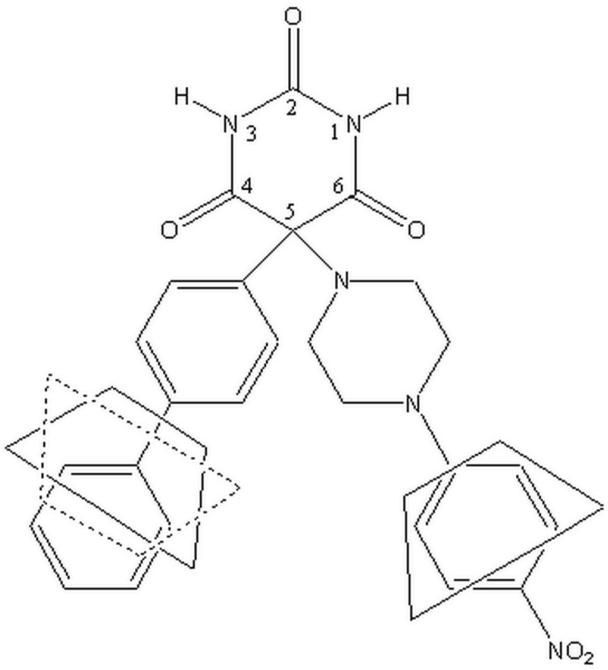

Figure 6: Representation of RO-DIMEB complex according to T-ROESY spectrum.

Molecular modeling

In aqueous solution, DIMEB and RO are in dynamic equilibrium with free CD, free RO, and RO/DIMEB complexes. Different conformations of the isolated molecules and of the complexes are mixed in the solution. Molecular modeling was performed to calculate some of the most energetically favorable conformations and possibly to confirm the ^{1}H-NMR observations. To perform calculations, RO and DIMEB geometries were reoptimized separately. RO presents many free rotation axes.

The piperazin cycle can take boat or chair conformation and sp3 nitrogen substituents can switch from the axial to the equatorial position. A DIMEB conformer has been built and optimized from an "opened" β-CD, in order to be able to load RO substituents. Since two subunits of RO can be included using DIMEB, five possible models were optimized.

To facilitate understanding, these different structures were numbered. For models B1 and B2, the biphenyl group is included inside the cavity of the DIMEB, whereas N1 and N2 correspond to the inclusion of the nitrophenyl group. The optimization of RO complexed by two DIMEBs was also investigated and was noted as B2N1. The suffixes "1" and "2" mean that DIMEB includes respectively the primary or the secondary hydroxyl face.

Results are presented as energetic outcomes expressed as complexation, deformation and interaction energies. Complexation energy (ΔE) is the difference between the energy of the complex and the sum of the energies of the RO and the DIMEB in their respective optimized equilibrium geometry. In this way, ΔE negative value means that the complex formation is energetically favorable. Deformation energy is the difference between the energy of partners of the complex at their respective equilibrium geometry and their energy at complex geometry. Interaction energy is the difference between the energy of the complex and the sum of the energies of both partners at their complex geometry.

This interaction energy can also be calculated as the sum of the deformation energy of both molecules and the complexation energy. The difference of free energy (ΔG) is positive for all the models; that is the reason why a contribution of energy is necessary to form these complexes. On optimized complexes, some interatomic distances were measured in order to show hydrogen bond formation between DIMEB and RO. In fact, a distance less than 3 Å between oxygen and hydrogen (aliphatic or not) allows the formation of a bond which improves complex stability (29,30). Energies, entropy and enthalpy values are presented in Table 2, while some interatomic distances are summarized in Table 3.

Table 2: Interaction, deformation and complexation energies in Kcal/mole (ΔS in calories/mole-Kelvin) with reference to the DIMEB and RO reoptimized.

	B1	B2	N1	N2	B2N1
Complexation energy					
ΔE	-8.073	-6.448	-5.412	-4.351	-9.934
ΔH	-6.554	-4.982	-4.066	-2.831	-6.806
ΔG	13.915	14.408	11.669	15.048	32.324
Deformation energy					
RO	-1.935	-1.595	-0.928	-0.480	-3.657
DIMEB Biphenyl	-1.506	-1.467			-1.644
DIMEB Nitro			-2.645	-5.725	-3.773
Interaction energy	-11.515	-9.509	-8.985	-10.555	-19.008

Table 3: Distance (Å) between some functions of RO and DIMEB able to form hydrogen bonds.

Inclusion mode	RO	DIMEB	Distance (Å)
B1	N-H 1	C-O- 6	2.305
	C=O 2	C-H 6	2.457
	C=O 2	C-H 6*	2.514
	N-H 3	C-O- 6	2.156
	C=O 4	C-H 6	2.353
B2	N-H 1	C-O- 2	2.381
	N-H 1	-OH 3	2.927
	C=O 2	C-H 2*	2.370
	C=O 4	C-H 2*	2.484
	C=O 4	C-H 2*	2.408
N1	C=O 4	C-H 6*	2.279
	C=O 6	C-H 6*	2.599
	C=O 6	C-H 6	2.415
N2	C=O 6	C-H 2*	2.355
B2N1	N-H 1	C-O- 2	2.309
	N-H 1	-OH 3	2.813
	C=O 2	-OH 3	2.284
	C=O 2	C-H 2*	2.498
	DIMEB biphenyl	**DIMEB nitrophenyl**	
	C-O- 2	C-H *6	2.500
	C-O- 3	C-H *6	2.466
	C-O- 3	C-H *6	2.296

Docking of biphenyl (B1 and B2)

The results show that both biphenyl inclusion modes form a stable complex (ΔE < 0). Even if B1 complexation energy is higher than B2 value, the entropy is similar for both complexes. It is interesting to note that B1 and B2 conformations lead to hydrogen bond formation between DIMEB and the barbituric ring (see Table 3), which consolidates the inclusion and improves interaction and, thereby, complexation energy values. These observations suggest that B1 and B2 conformations are stable complex configurations that can exist with the same probability.

Table 4: Composition of RO nebulizable solutions at 300 and 30 μg/mL.

	Formulation name			
	HP300	RAM300	HP30	RAM30
RO	300 μg	300 μg	30 μg	30 μg
HP-β-CD	43 mg		4.7 mg	
RAMEB		19.7 mg		2.62 mg
NaCl	q.s. 286 mOsm/kg			
Water for injection	a.d. 1 ml			

Docking of nitrophenyl (N1 and N2)

In contrast to the docking of biphenyl, N1 and N2 do not give equivalent results. In fact, ΔE values show that N1 is more stable than N2. It can also be observed for N2 that DIMEB needs twice as much energy to lose its shape in order to complex the nitrophenyl group. Concerning H-bond formation, Figure 7 shows that, in contrast with N1, the barbituric ring orientation in N2 does not allow the formation of many H-bonds with DIMEB. These results demonstrate that N1 is more favorable than N2 and confirm the ^{1}H-NMR observations.

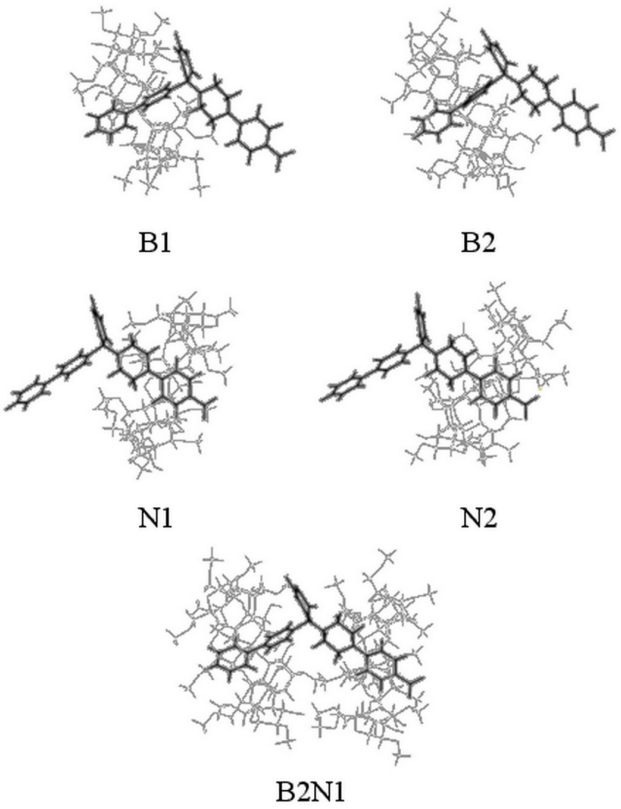

Figure 7: The five inclusion modes of RO: B1, B2, N1, N2 and B1N2

Docking of biphenyl and nitrophenyl (B2N1)

As expected, this complex formation exhibits great entropy variation. The closeness of partners in B2N1 requires that RO and DIMEB undergo some geometry deformations to form the complex, thereby explaining the high level of deformation energies. The interatomic measurements again show H-bonds between the barbituric ring and DIMEB, but surprisingly between both DIMEBs too. All these interactions contribute to complex stability, which is confirmed by the ΔE value.

Development of RO nebulizable solutions and study of their stability

300 and 30 μg/mL RO solutions were prepared with HP-β-CD and RAMEB (see Table 4). Both CDs were selected taking into consideration their solubilizing properties and their compatibility with pulmonary administration (21). Suitable amounts of CD were calculated by solving equations 3 and 4 from the stability constants obtained after phase solubility studies (see Table 1).

$$Y = \beta_0 + \beta_1.t + \beta_2.T + \beta_3.CD + \beta_4.r + \beta_5.t^2 + \beta_6.t.r + \beta_7.t^2.r + \beta_8.CD.r + \beta_9.t.CD.r + \beta_{10}.t^2.CD.r + \beta_{11}.t.T + \beta_{12}.t^2.T \quad \text{Eq.4}$$

Y corresponds to RO concentration (μg/mL)
t corresponds to time (0, 0.25, 1, 3, 6 and 9 months)
T corresponds to temperature (4 or 25°C)
CD corresponds to CD type (HP-β-CD = 1, RAMEB = 0)
r corresponds to the percentage of 1:2 complex *v.s.* 1:1 complex in solution (RAM30 4.4%, HP30 5.6%, RAM300 33.4% and HP300 36.4%)

It can be noted that CD concentrations (4 and 30 mM for HP-β-CD, 2 and 15 mM for RAMEB), needed to solubilize RO, are compatible with aerosol production (21).

Table 5: Percentage of droplets in the range of 0.5 to 5 μm, mass median aerodynamic diameter (MMAD) and geometric standard deviation (GSD).

Sol.	% of droplets (0.5 - 5.79 μm)		MMAD (μm)		GSD	
	mean	Std	mean	Std	mean	Std
RAM30	69.34	1.08	5.01	0.08	1.48	0.04
RAM300	64.5	0.85	5.22	0.07	1.34	0.03
HP30	64.58	0.77	5.55	0.16	1.45	0.01
HP300	67.38	0.85	5.46	0.11	1.39	0.01

HPLC analysis of nebulizable solutions prepared as described by phase solubility study (Figure 8a) or after steam sterilization process (Figure 8b) shows that those solutions exhibit identical chromatograms and RO peak area values, which demonstrates that the steam sterilization process does not provoke any detectable RO degradation. Chromatographic analysis of stored RO solutions shows that some unidentified peaks, which do not interfere with the RO peak, can be detected (Figure 7c).

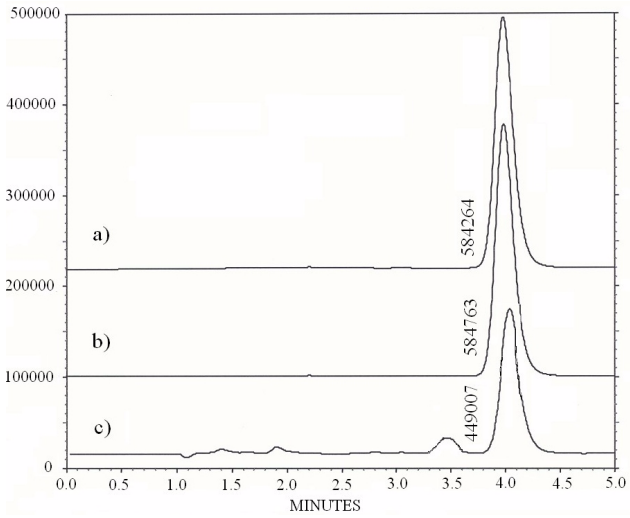

Figure 8: Chromatograms obtained after injection of 30μg/mL RO solutions freshly prepared with RAMEB as described by the phase solubility study (a), by steam sterilization process (b) and after 9 months storage at 25°C (c). The value mentioned on the left of the peak corresponds to its area.

Those peaks probably correspond to RO degradation products, which cannot be quantified by this HPLC method. Droplet size data of the nebulized solutions are summarized in Table 5.

For all solutions, the percentage of droplets in the range of 0.5--5 μm is close to 45%. Those size distributions are compatible with an appropriate human pulmonary deposition. The RO content in nebulizable solutions according to time is plotted in Figure 9.

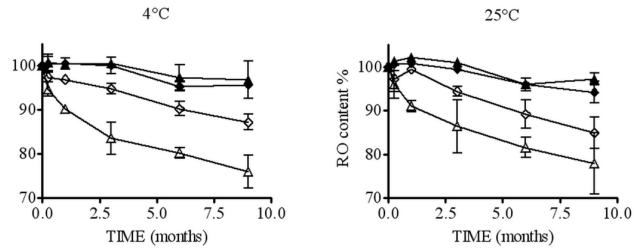

Figure 9: Representation of RO content in HP300 (◆), HP 30 (✧), RAM300 (▲)and RAM30 (Δ) according to time at two temperatures.

These results show that higher CD concentrations (RAM300 and HP300) are more effective in protecting RO in solution. Unfortunately, the CD concentration is not correlated with the ratio [CD]/[RO]. In fact, RAM300 and HP300 exhibit a lower ratio [CD]/[RO] than RAM30 and HP30, which is incompatible with a potential CD protective effect. For this reason, it is better to express CD concentration as the percentage of 1:2 complex *vs.* 1:1 complex (calculated by eq. 3 and 4), which increases with CD concentration.

In order to investigate how some parameters influence RO solution stability, a statistical analysis was performed on a general linear mixed model described by equation 4. This statistical analysis determines the values of all β_x and their significance in equation 4.

Statistical results (Table 6) confirm that solutions are not stable ($\beta_1 < 0$) and that degradation of RO solution does not follow zero order kinetics (P value of $\beta_5 <$ 0.05).

Table 6: Statistical analysis of equation 4.

Effect	Estimation	Error type	t value	P value
β_0	-10.2132	1.9765	-5.17	<0.0001
β_1	-1.40076	0.5	-2.82	0.0111
β_2	-0.1241	0.07317	-1.70	0.1061
β_3	-7.3952	2.1983	-3.36	0.0033
β_4	9.18822	0.07209	127.36	<0.0001
β_5	0.1609	0.06408	2.51	0.0212
β_6	0.03903	0.01883	2.07	0.0521
β_7	0.00881	0.002414	-3.65	0.0017
β_8	-0.3034	0.09402	-3.24	0.0043
β_9	-0.0193	0.01864	-1.04	0.3134
β_{10}	0.000371	0.002389	0.16	0.8781
β_{11}	0.00325	0.0022	0.15	0.8841
β_{12}	-0.00235	0.002819	-0.83	0.4142

Concerning the percentage of 1:2 complex, the analysis shows that this is a critical parameter. The higher this percentage is, the greater the RO stability in solution. Even though the RO degradation mechanism is not yet understood, a hypothesis can explain this phenomenon. In the case of 1:1 complex conformation, only one barbituric group is inside the CD cavity, whereas with a 1:2 inclusion, the whole of RO is closely protected by both CDs.

If the CD type has an effect on RO solution stability (P value of $\beta_3 < 0.05$), it is the interaction between CD and r, in particular, which has the biggest impact (P values of β_8 and $\beta^4 < 0.05$). In fact, HP-β-CD can be considered as more effective than RAMEB to protect RO, but only if the percentage of 1:2 complex is equal or greater than the RAMEB one. It may also be noted that storage temperatures (4 or 25°C) do not affect RO solution stability (P value of $\beta_2 > 0.05$). All these results allow the optimization of the formulation of a nebulizable solution of RO. Thus, to prepare solutions whatever the RO concentration, it is preferable to use HP-β-CD with the higher concentration, which must be compatible with the production of a respirable aerosol (21). The solutions do not require storage in a refrigerator.

CONCLUSIONS

This study shows that RO aqueous solubility can be improved by the use of CDs (up to 12 mg/ml with RAMEB at 200 mM). RAMEB, HP-β-CD and β-CD form a mixture of 1:1 and 1:2 complexes with high 1:1 stability constant values, whereas γ-CD shows a weak affinity for RO, probably because it has too large a cavity. The ^{1}H-NMR study demonstrated that DIMEB interacts with RO through the nitrophenyl and biphenyl groups with preferential inclusion directions. The molecular modeling study demonstrated that inclusion modes observed with ^{1}H-NMR were energetically possible and that these complexes are notably stabilized by H-bonds formation between complex partners. The stability study demonstrated that RO nebulizable solutions are not stable (RO content was < 95% after 9 months). It was also demonstrated that the proportion of 1:2 complex in solution is the most critical parameter on RO stability and that HP-β-CD is the most protective cyclodextrin.

ACKNOWLEDGMENTS

This work has been supported financially by the Ministry of Walloon Region. G. Piel an D. Cataldo are postdoctoral researchers supported by the F.N.R.S., Brussels, Belgium. G. Dive is a research associate of the F.N.R.S., Brussels, Belgium. The C.I.P. thanks the Belgian program on Interuniversity Poles of Attraction initiated by the Federal office for Scientific, Technical and Cultural Affaires (PAI n°P5/33) for financial support and the FNRS for the access to the SGI computer.

REFERENCES

[1] Massova, I.; Kotra, L. P.; Fridman, R.; Mobashery, S. Matrix metalloproteinases: structures, evolution, and diversification. *FASEB J.,* 12: 1075-1095, 1998

[2] Beckett, R.; Davidson, A. H.; Drummond, A. H.; Huxley, P.; Whittaker, M. Recent advances in matrix metalloproteinase inhibitor research. *Drug Discov. Today*, 1: 16-26, 1996

[3] Glasspool, R. M.; Twelves, C. J. Matrix metalloproteinase inhibitors: past lessons and future prospects in breast cancer. *The Breast*, 10: 368-378, 2001

[4] Janusz, M. J.; Bendele, A. M.; Brown, K. K.; Taiwo, Y. O.; Hsieh, L.; Heitmeyer, S. A. Induction of osteoarthritis in the rat by surgical tear of the meniscus: Inhibition of joint damage by a matrix metalloproteinase inhibitor. *Osteoarthr. Cartilage*, 10: 785-791, 2002

[5] Kim, J. H.; Lee, S. Y.; Bak, S. M.; Suh, I. B.; Lee, S. Y.; Shin, C.; Shim, J. J.; In, K. H.; Kang, K. H.; Yoo, S. H. Effects of matrix metalloproteinase inhibitor on LPS-induced goblet cell metaplasia. *Am. J. Physiol. Lung Cell. Mol. Physiol*., 287: 127-133, 2004

[6] Sivak, J. M.; Fini, M. E. MMPs in the eye: emerging roles for matrix metalloproteinases in ocular physiology. *Prog. Retin. Eye Res.*, 21: 1-14, 2002

[7] Bousquet, J.; Jeffery, P. K.; Busse, W. W.; Johnson, M.; Vignola, A. M. Asthma. From bronchoconstriction to airways inflammation and remodeling. *Am. J. Respir. Crit. Care Med.,* 161: 1720-1745, 2000

[8] Vignola, A. M.; Mirabella, F.; Costanzo, G.; Di Giorgi, R.; Gjomarkaj, M.; Bellia, V.; Bonsignore, G. Airway remodeling in asthma. *Chest*, 123: 417S-422S, 2003

[9] Atkinson, J. J.; Senior, R. M. Matrix metalloproteinase-9 in lung remodeling. *Am. J. Respir. Cell. Mol. Biol.,*. 28: 12-24, 2003

[10] Cataldo, D.; Munaut, C.; Noel, A.; Frankenne, F.; Bartsch, P.; Foidart, J. M.; Louis, R. MMP-2 and MMP-9-linked gelatinolytic activity in the sputum from patients with asthma and chronic obstructive pulmonary disease. *Int. Arch. Allergy Immunol,*. 123: 259-267, 2000

[11] Cataldo, D. D.; Gueders, M. M.; Rocks, N.; Sounni, N. E.; Evrard, B.; Bartsch, P.; Louis, R.; Noel, A.; Foidart, J. M. Pathogenic role of matrix metalloproteases and their inhibitors in asthma and chronic obstructive pulmonary disease and therapeutic relevance of matrix metalloproteases inhibitors. *Cell. Mol. Biol*, 49: 875-884, 2003

[12] Kim, J. H.; Lee, S. Y.; Bak, S. M.; Suh, I. B.; Lee, S. Y.; Shin, C.; Shim, J. J.; In, K. H.; Kang, K. H.; Yoo, S. H. Effects of matrix metalloproteinase inhibitor on LPS-induced goblet cell metaplasia. *Am. J. Physiol. Lung Cell Mol. Physiol.* , 287: 127-133,2004

[13] Beckett, R.; Davidson, A. H.; Drummond, A. H.; Huxley, P.; Whittaker, M. Recent advances in matrix metalloproteinase inhibitor research. *Drug Discov. Today*, 1: 16-26, 1996

[14] Grams, F.; Brandstetter, H.; D'Alo, S.; Geppert, D.; Krell, H. W.; Leinert, H.; Livi, V.; Menta, E.; Oliva, A.; Zimmermann, G.; Gram, F.; Brandstetter, H.; D'Alo, S.; Geppert, D.; Krell, H. W.; Leinert, H.; Livi, V. E.; Oliva, A.; Zimmermann, G. Pyrimidine-2,4,6-Triones: a new effective and selective class of matrix metalloproteinase inhibitors. *Biol. Chem.,* 382: 1277-1285, 2001

[15] Maquoi, E.; Sounni, N. E.; Devy, L.; Olivier, F.; Frankenne, F.; Krell, H. W.; Grams, F.; Foidart, J. M.; Noel, A. Anti-invasive, antitumoral, and antiangiogenic efficacy of a pyrimidine-2,4,6-trione derivative, an orally active and selective matrix metalloproteinases inhibitor. *Clin. Cancer Res.,* 10: 4038-4047, 2004

[16] Lein, M.; Jung, K.; Ortel, B.; Stephan, C.; Rothaug, W.; Juchem, R.; Johannsen, M.; Deger, S.; Schnorr, D.; Loening, S.; Krell, H. W. The new synthetic matrix metalloproteinase inhibitor (Roche 28-2653) reduces tumor growth and prolongs survival in a prostate cancer standard rat model. *Oncogene*, 21: 2089-2096, 2002

[17] Dubowski, K. M. Studies in breath-alcohol analysis: biological factors. *Z. Rechtsmed.,* 76: 93-117, 1975

[18] Suber, R. L.; Deskin, R.; Nikiforov, I.; Fouillet, X.; Coggins, C. R. Subchronic nose-only inhalation study of propylene glycol in Sprague-Dawley rats. *Food Chem. Toxicol.,* 27: 573-583,1989

[19] Del Valle, E. M. M. Cyclodextrins and their uses: a review. *Prog. Biochem. Biophys.*, 39: 1033-1046, 2004

[20] Frömming, K. H.; Szejtli, J. Cyclodextrins in Pharmacy. Kluwer Academic Publishers: Dordrecht, 2004.

[21] Evrard, B.; Bertholet, P.; Gueders, M.; Flament, M.-P.; Piel, G.; Delattre, L.; Gayot, A.; Leterme, P.; Foidart, J.-M.; Cataldo, D. Cyclodextrins as a potential carrier in drug nebulization. *J. Control. Release*, 96: 403-410, 2004

[22] Higuchi, T.; Connors, K. A. Phase solubility technics. *Adv. Anal. Chem. Instrum.* 4: 117-212, 1965

[23] Frisch, M. J, Trucks, G.W.; Schlegel, H.B.; Scuseria, G.E.; Robb, M.A.; Cheeseman, J.R.; Zakrzewski, V.G.; Montgomery, J.A.; Stratmann, R.E; Burant, J.C.; Dapprich, S.; Millam, J.M.; Daniels, A.D.; Kudin, K.N.; Strain, M.C.; Chen, W.; Farkas, O.;

Tomasi, J.; Barone, V.; Cossi, M.; Cammi, R.; Mennucci, B.; Pomelli, C.; Adamo, C.; Clifford, S.; Ochterski, J.; Petersson, G.A.; Ayala, P.Y; Cui, Q.; Morokuma, K.; Malick, D.K.; Rabuck, A.D.; Raghavachari, K.; Foresman, J.B.; Ciolowski, J.; Oritz, J.V.; Baboul, A.G.G; Stefanov, B.B.; Liu, G.; Liashenko, A.; Piskorz, P.; Komaromi, I.; Gomperts, R.; Martin, R.L.; Fox, D.J.; Keith, T.; Al-Laham, M.A; Peng, C.Y.; Nanyakkara, A.; Gonzalez, C.; Challacombe, M.; Gill, P.M.W.; Jonhson, B.; Wong, M.W.; Andres, J.L.; Head-Gordon, M.; Replogle, E.S.; Pople, J.A. Gaussian 98. [A.7]. 1998. Inc. Pittsburgh PA.

[24] MC Quarrie, D. A. Statistical Thermodynamics. New-York, 1973.

[25] Piel, G.; Dive, G.; Evrard, B.; Van Hees, T.; de Hassonville, S. H.; Delattre, L. Molecular modeling study of β - and γ-cyclodextrin complexes with miconazole. *Eur. J. Pharm. Sci.*, 13: 271-279, 2001

[26] Henry de Hassonville, S.; Dive, G.; Evrard, B.; Barillaro, V.; Bertholet, P.; Delattre, L.; Piel, G. Application of molecular modeling to the study of cyproterone acetate stability in the presence of cyclodextrin derivatives. *J. Drug Deliv. Sci. and Technology*, 14: 357-362, 2004

[27] The European Agency for the Evaluation of Medicinal Products. ICH Q1A (R2) Stability testing guidelines: Stability testing of new drug substances and products. Note for guidance on stability testing : Stability testing of new drug substances and products (Revision2). 2003.

[28] Djedaïni, F.; Perly, B. Nuclear Magnetic Resonance of Cyclodextrins, Derivatives and Inclusion Compounds. In New Trends in Cyclodextrins and Derivatives, Edition de la Santé ed.; Paris, 1990.

[29] Dive, G.; Dehareng, D.; Ghuyen, J. M. Energy analysis on small to medium sized H-bonded complexes. *Theor. Chim. Acta*, 85: 409-421, 1993

[30] Thomas, A.; Benhabiles, N.; Meurisse, R.; Ngwabije, R.; Brasseur, R. Pex, analytical tools for PDB files. II. H-Pex: noncanonical H-bonds in alpha-helices. *Proteins*, 43: 37-44, 2001